Food Chemistry: X 21 (2024) 101090

Contents lists available at ScienceDirect

Food Chemistry: X

journal homepage: www.sciencedirect.com/journal/food-chemistry-x

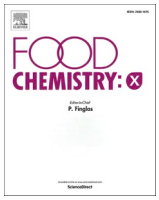

Analytical Methods

One-pot derivatization/magnetic solid-phase extraction coupled with liquid chromatography-fluorescence detection for the rapid determination of sulfonamide residues in honey

Nian Shi [a,*], Yuwei Liu [b], Wenxuan Li [b], Shumei Yan [a], Lei Ma [c], Xia Xu [b,c], Di Chen [b,c]

[a] Physics Diagnostic Division, The First Affiliated Hospital of Zhengzhou University, Zhengzhou 450052, China
[b] Key Laboratory of Targeting Therapy and Diagnosis for Critical Diseases of Henan Province, and School of Pharmaceutical Sciences, Zhengzhou University, Zhengzhou 450001, China
[c] Zhengzhou Research Base, National Key Laboratory of Cotton Bio-breeding and Integrated Utilization, Zhengzhou University, Zhengzhou 450000, China

ARTICLE INFO

Keywords:
One-pot derivatization/magnetic solid-phase extraction
Fe_3O_4/MWCNTs-OH
Sulfonamides
Liquid chromatography-fluorescence detection
Honey

ABSTRACT

Consuming foods with excess sulfonamide residues threatens human health, underscoring the importance of their detection in food. This study presents an innovative one-pot derivatization/magnetic solid-phase extraction (OPD/MSPE) method for sulfonamides analysis. This approach integrates the derivatization and extraction steps into a single process. The sample solution, along with the derivatization reagent fluorescamine and the sorbent magnetic hydroxyl multi-walled carbon nanotubes, is mixed and vortexed for 3 min. This procedure simultaneously conducts derivatization and extraction, with easy phase separation using an external magnet. This streamlined sample preparation method is completed in only 5 min and, when combined with liquid chromatography-fluorescence detection (LC-FLD), demonstrates excellent linearity ($R^2 > 0.99$) and satisfactory detection limits (0.004–0.04 ng/g) for the quantification of nine sulfonamides in honey samples. The proposed OPD/MSPE-LC-FLD method is distinguished by its simplicity, rapidity, high sensitivity, and specificity, making it an outstanding advancement in the field of food safety analysis.

1. Introduction

Sulfonamides (SAs) are synthetic antimicrobial agents extensively utilized in both human and animal medicine owing to their affordability, high efficiency, and broad-spectrum antibacterial activity (Dai et al., 2023; Ning et al., 2022). However, SAs are not fully degraded in humans and animals. Their prototype drugs can enter the environment via urine and feces, contributing to soil and water pollution (Chen et al., 2018). The pervasive use of SAs lead to their residue in the environment and animal-derived products. Consequently, these residues can accumulate in the human body through the food chain, causing a range of adverse reactions, including drug resistance, allergies, and damage to the urinary system (Duan et al., 2022). Therefore, establishing a reliable method for detecting SA residues in animal-derived food is crucial for public health and environmental safety.

Honey is globally esteemed as a natural and healthful product, prompting various countries to establish maximum residue limits (MRLs) for SA drugs to safeguard its safety. In the European Union, the use of antimicrobials for treating honeybees is prohibited, resulting in no specific MRLs for sulfonamides in honey (Zhang et al., 2019). In contrast, China has specified an MRL of 50 μg/kg for each sulfonamide. Moreover, some countries have set action limits or tolerance thresholds for antibiotics in honey (Baeza Fonte et al., 2018). For instance, Belgium has a limit of 20 μg/kg, while Great Britain's limit is 50 μg/kg, both for the total sulfonamides content (Bonerba et al., 2021; Zhang et al., 2019). Additionally, in certain regions where legislation is less defined, a strict zero-tolerance policy for antibiotic residues in honey is often enforced.

For the present, numerous methods, such as electrochemistry, digital image measurement, fluorescence spectroscopy, ultraviolet spectroscopy, and chromatography, have all been employed to detect SAs (Xie et al., 2020). Among these, liquid chromatography (LC) is particularly favored for its high selectivity and commendable reproducibility. Nonetheless, the direct and precise analysis of SAs using LC can be arduous due to the intricate nature of the sample matrix and the minute concentrations of SA residues. Consequently, an effective sample pretreatment, encompassing extraction, purification, and derivatization, is

* Corresponding author.
E-mail address: 13503823257@163.com (N. Shi).

https://doi.org/10.1016/j.fochx.2023.101090
Received 28 July 2023; Received in revised form 12 December 2023; Accepted 18 December 2023
Available online 21 December 2023

essential before conducting LC analysis.

In recent years, the integration of chemical derivatization and extraction technology has become increasingly prevalent in food analysis (Cao et al., 2019; Luo et al., 2021). This integrated approach allows for the enrichment and purification of analytes, significantly improving the selectivity and sensitivity of methods. Traditionally, in SA analysis, extraction and derivatization are performed either independently or in succession. However, this often results in prolonged, labor-intensive derivatization stages (Dmitrienko et al., 2015; Xie et al., 2020). Further, additional steps involving sample transfer can lead to analytical inaccuracies, affecting test result reliability. Consequently, developing a new sample pretreatment process that streamlines the integrated procedure and reduces the overall duration for SA analysis is of critical importance.

This study aims to develop a rapid, sensitive and selective method for determination of SAs. To achieve this, fluorescamine (FSA), a widely used fluorescent derivatization reagent (Li et al., 2020; Yang et al., 2018), was employed to transform SAs into derivatives with enhanced sensitivity and selectivity for fluorescence detection (FLD). Magnetic hydroxyl-functionalized multi-walled carbon nanotubes (Fe_3O_4/MWCNTs-OH) were selected as the sorbent, leveraging their ability to selectively extract FSA-labeled SA derivatives through hydrophobic and π-π interactions from complex food matrices. Thus, a novel one-pot derivatization/magnetic solid-phase extraction (OPD/MSPE) method was introduced, facilitating simultaneous derivatization and extraction in SA analysis. The primary factors influencing the derivatization/extraction efficiency were optimized, and key quantitative parameters, including linearity, detection limit, accuracy, and precision, were evaluated. In conjunction with LC-FLD, the OPD/MSPE method was also applied to analyze SA residues in honey samples. The performance of the integrated OPD/MSPE-LC-FLD method was thoroughly compared with other reported techniques, highlighting its unique characteristics and advantages.

2. Experimental

2.1. Chemicals and reagents

Fluorescamine (FSA), sulfonamide (SA), sulfadiazine (SDZ), sulfamethoxazole (SMX), and sulfamethazine (SMZ) were purchased from Rhawn Biotechnology Co., Ltd. (Shanghai, China). Sulfamethoxazole (SDM), sulfaguanidine (SGN), and sulfamethazine (SMD) were obtained from Titan Biotechnology Co., Ltd. (Shanghai, China). Sulfabenzamide (SB), sulfaquinoxaline sodium (SQX), and sulfamonomethoxine (SMM) were purchased from Bide Biotechnology Co., Ltd. (Shanghai, China). The chemical structures of the nine studied SAs are shown in Fig. 1. Sodium acetate and hydroxylated multi-walled carbon nanotubes were provided by Aladdin Biochemical Technology Co., Ltd. (Shanghai, China). Acetic acid (≥99 %) was obtained from Tianjin Komeo Chemical Reagent Co., Ltd. (Tianjin, China). LC-grade methanol (MeOH) and acetonitrile (ACN) were provided by Sinopharm Chemical Reagent Co., Ltd. (Shanghai, China). Ultrapure water was obtained from a Milli-Q water purification system (Millipore, Billerica, MA, USA). Submicron-sized magnetic particles (Fe_3O_4) were purchased from Nangong Yingtai Metal Material Co., Ltd. Hydroxyl-functionalized multi-walled carbon nanotubes (MWCNTs-OH) (purity; 95 wt%, outer diameter 30–50 nm, inner diameter 5–12 nm, and length 10–20 μm) were purchased from Aladdin Co., Ltd. (Shanghai, China).

Individual stock solutions of SAs were prepared by dissolving accurately weighed amounts of solid powder in ACN to achieve a concentration of 1.0 mg/mL. A mixed standard solution of SAs (100 μg/mL) was formulated from these individual stock solutions. All stock solutions were stored at −20 °C in the dark until use. The standard working solutions were made by diluting the mixed stock solution with purified water to the desired concentrations of SAs. The FSA solution was prepared by dissolving an accurately weighed amount of solid powder in ACN to reach a concentration of 5.0 mg/mL. It was stored in dark glass bottles at −20 °C and used within 3 months. The acetic acid buffer solution (250 mM, pH 3.5) was freshly prepared weekly using acetic acid and sodium acetate for the derivatization reaction.

Eight varieties of honey samples were purchased from a local

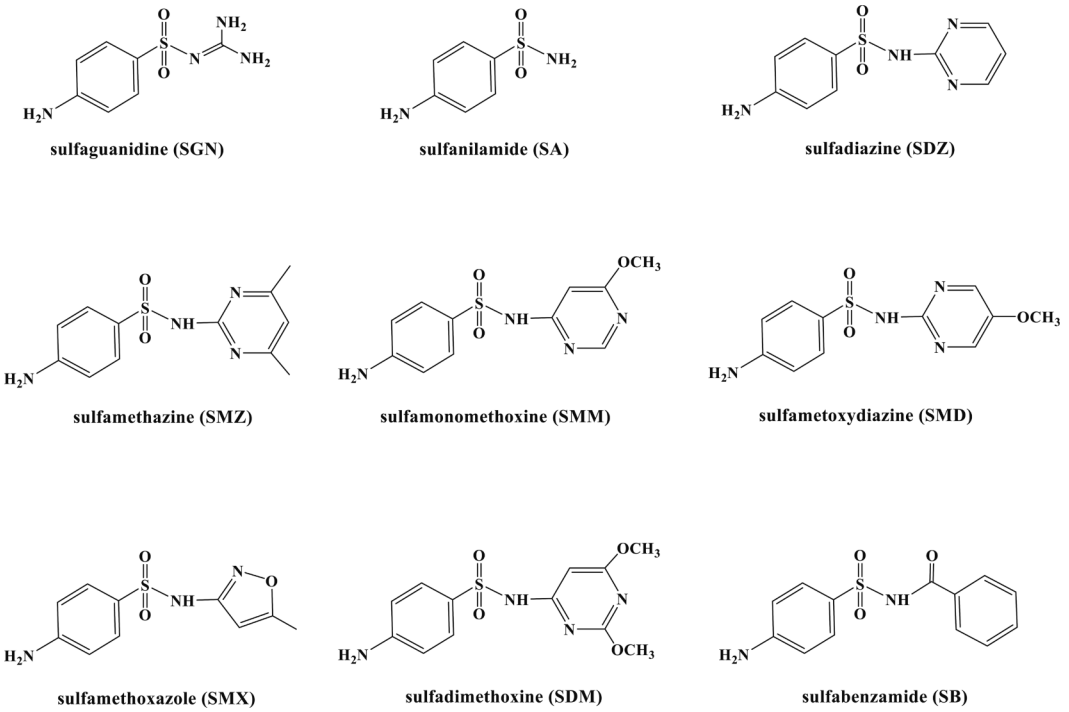

Fig. 1. The chemical structures of the sulfonamides studied.

supermarket (Zhengzhou, China). These included linden honey, jingtiao honey, jujube honey, buckwheat honey, honeysuckle honey, Chinese wolfberry honey, acacia honey, and hundred flowers honey. Detailed information about these honey samples is available in the Supporting Information.

2.2. Preparation of Fe_3O_4/MWCNTS-OH

The Fe_3O_4/MWCNTs-OH material was prepared using an "aggregate wrap" strategy reported by Feng's group (Zheng et al., 2016). Specifically, 8.0 g of Fe_3O_4 and 2.0 g of MWCNTs-OH were accurately weighed and ground together in a mortar until a homogeneous fine powder was achieved. This powder, termed Fe_3O_4/MWCNTs-OH, was employed in the subsequent OPD/MSPE procedure.

A Nicolet IS10 Fourier Transform Infrared (FT-IR) spectrometer (Thermo Scientific, San Jose, USA) was utilized to characterize Fe_3O_4/MWCNTs-OH. Scanning Electron Microscopy (SEM) imaging was performed with a Sigma300 SEM (ZEISS, Germany). Magnetic characterization was conducted using SQUID based vibrating sample magnetometer (MPMS 3, Quantum Design). Nitrogen adsorption–desorption isotherms at 77 K were measured using Micromeritics ASAP 2460 adsorption equipment (Micromeritics Instruments, USA). The specific surface area of the samples was calculated using the Brunauer-Emmett-Teller (BET) method, based on nitrogen adsorption isotherm data at relative pressures ranging from 0.05 to 0.3.

2.3. Sample pretreatment

A 5.0 g portion of the honey sample was placed in a 15 mL centrifuge tube, followed by the addition of 10.0 mL of ACN. After undergoing ultrasonic treatment for 20 min and centrifugation at 10,000g for 3 min, the supernatant ACN layer was collected and evaporated to dryness under a stream of nitrogen gas. The residue was then redissolved in 1.5 mL of water for subsequent use. Standard solutions of SAs at a concentration of 20 ng/mL, were prepared by diluting the mixed stock solution with purified water. These were used both to optimize extraction conditions and to validate the methodology.

2.4. One-pot derivatization/magnetic solid-phase extraction pretreatment procedure

The OPD/MSPE process, as depicted in Fig. 2, was carried out as follows. Initially, 1.5 mL of the sample solution, 200 μL of the sodium acetate buffer solution (250 mM, pH 3.5), 50 μL of FSA (12 mg/mL), and 4 mg of Fe_3O_4/MWCNTs-OH materials were sequentially added to a 2 mL centrifuge tube. The mixture was then vortexed for 3 min to facilitate simultaneous derivatization and extraction. After the reaction was completed, the supernatant was separated and discarded with the aid of an external magnet. Subsequently, 250 μL of acetone was added to the tube, which was then vortexed for 2 min to elute the compounds. The eluate was collected using an external magnet. Finally, the collected eluate was diluted with an equal volume of water and then directly subjected to LC-FLD analysis.

2.5. LC-FLD analysis

An ACQUITY e2695 high-performance liquid chromatography system coupled with a fluorescence detector (Waters Corp., Milford, MA, USA) was utilized for the analysis of SAs. The LC separation was achieved using an Agilent 5 TC-C18 column (150 × 4.6 mm, 5 μm). The mobile phase was composed of (A) 0.1 % formic acid in water and (B) 0.1 % formic acid in acetonitrile, with a flow rate of 1.0 mL/min. The gradient program was as follows: 0–15 min, 70 % A; 15–20 min, 68 % A; 20–40 min, 58 % A; 40–45 min, 70 % A; 45–50 min, 70 % A (isocratic). The fluorescence detector (FLD) had excitation and emission wavelengths set at 395 nm and 491 nm, respectively. The column temperature was maintained at 30 °C. The autosampler's temperature was set at 4 °C and the sample injection volume was 20 μL. Each analysis time run lasted for a total of 50 min. Data acquisition and processing were carried out using the Waters Empower 3.1 software.

3. Results and discussion

3.1. The feasibility study and performance assessment of OPD/MSPE

Due to the typically low levels of sulfonamide residues in food, establishing sensitive analysis methods is necessary. By using FSA to derivatize SAs into fluorescent-responsive derivatives, the detection sensitivity can be significantly enhanced. Moreover, the hydrophobicity of the derived products increases, facilitating the extraction process. The extraction material's excellent dispersibility in the solution allows for rapid extraction and desorption processes. MWCNTs-OH was chosen as the adsorbent due to its superior dispersibility in both aqueous and organic samples. To further optimize the procedure and bypass tedious laborious centrifugation steps, magnetic MWCNTs-OH (Fe_3O_4/MWCNTs-OH) was synthesized using a convenient "aggregate wrap" strategy (Zheng et al., 2016).

SEM images reveal that Fe_3O_4 particles exhibit a distinct cubic morphology (Fig. S1A), while MWCNTs-OH displays a characteristic entangled fibrous structure (Fig. S1B). The integration of these materials into the Fe_3O_4/MWCNTs-OH composite is evidenced by SEM images that depict Fe_3O_4 nanoparticles uniformly dispersed and affixed to the

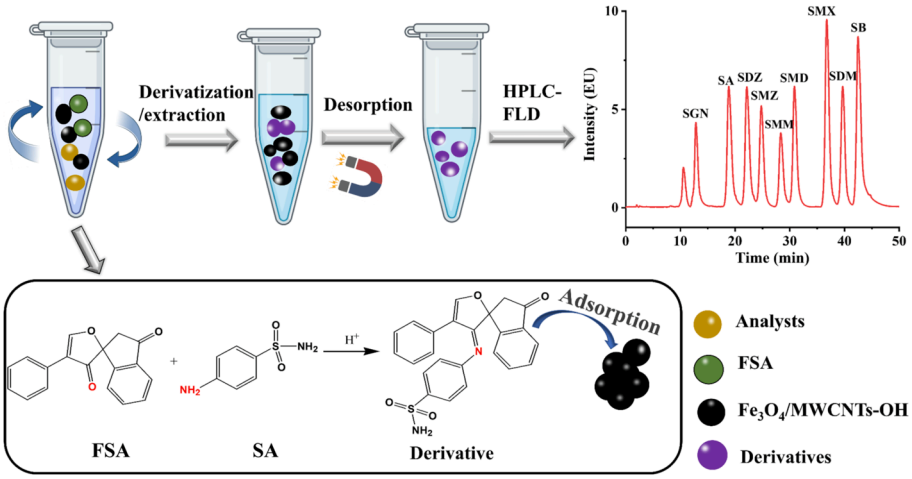

Fig. 2. Schematic diagram of the OPD/MSPE procedure for SAs analysis.

MWCNTs' surfaces (Fig. S1C), indicative of successful composite formation. The FTIR spectrum of Fe_3O_4/MWCNTs-OH showcases distinct absorption bands representative of both constituents. The Fe_3O_4 spectrum is marked by a Fe-O stretching band at 574 cm^{-1} (Fig. S2, blue line), while MWCNTs-OH features a broad band around 3430 cm^{-1} (Fig. S2, red line), denoting O—H stretching vibrations associated with hydroxyl groups. Additional peaks at approximately 1600 cm^{-1} and 1350 cm^{-1} correspond to C═C stretching and aromatic C═O stretching vibrations, respectively. The composite's spectrum integrates these bands, substantiating the co-presence of Fe_3O_4 and MWCNTs-OH and affirming the successful synthesis of Fe_3O_4/MWCNTs-OH (Fig. S2, grey line).

Nitrogen adsorption–desorption isotherms were utilized to characterize the surface area and pore size distribution of the Fe_3O_4/MWCNTs-OH composite. As depicted in Fig. S3A, the material demonstrated a BET surface area of 27.2 m^2/g. Additionally, the pore size distribution, illustrated in Fig. S3B, revealed a distinct peak, denoting a concentration of pores around the size of 2.5 nm. This suggests a predominantly uniform mesoporous architecture, which is advantageous for adsorptive applications due to the enhanced surface area accessible for analyte interaction.

The magnetization curves of Fe_3O_4/MWCNTs-OH at room temperature shown in Fig. 3A displayed a saturation magnetization intensity of 64 emu/g. This intensity, while slightly lower than that of pure Fe_3O_4, demonstrates significant magnetic responsiveness. In contrast, the magnetization of MWCNTs-OH is almost negligible, indicating minimal inherent magnetization and a lack of magnetic properties without the presence of Fe_3O_4. Consequently, Fe_3O_4/MWCNTs-OH facilitates effective solid–liquid separation under applied magnetic fields across various solvents, as illustrated in Fig. 3B. This confirms the composite material's efficacy as a magnetic sorbent.

The efficacy of the OPD/MSPE method was examined by analyzing standard aqueous solutions with nine SAs at a concentration of 20.0 ng/mL, as well as blank aqueous solutions without SAs. The derivatives of the SAs (20.0 ng/mL) standard aqueous solution served as a reference. The results showcased that all nine FSA-SAs were effectively detected (Fig. 4, curve B), with their retention times aligning with those of the derivatives from the standard analyte solution (Fig. 4, curve A). Additionally, the signal intensity was notably heightened using the OPD/MSPE method. No interfering signals were discernible in the peaks of the blank solution (Fig. 4, curve C), indicating the proposed OPD/MSPE method's efficacy for the purification and enrichment of SAs.

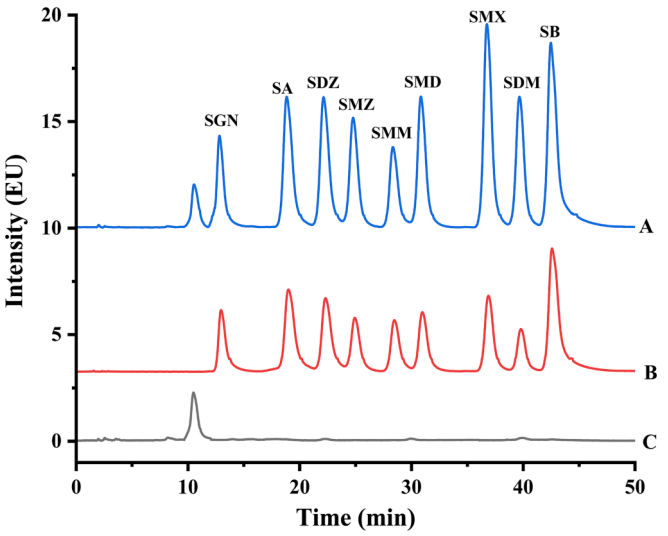

Fig. 4. The LC-FLD chromatogram of (A) SAs-free aqueous solution treated with OPD/MSPE, (B) SAs aqueous solution (20 ng/mL) treated with FSA derivatization only, and (C) SAs aqueous solution (20 ng/mL) treated with OPD/MSPE.

3.2. Optimization of OPD/MSPE conditions

The primary factors affecting the extraction efficiency were meticulously optimized to ascertain the best extraction conditions. These factors encompassed the concentration of FSA, pH of the buffer solution, derivatization/extraction time, quantity of Fe_3O_4/MWCNTs-OH sorbent, type and volume of the desorption solvent, and desorption time. For the optimization of these conditions, mixed standard aqueous solutions of SAs, each with a concentration of 2.0 ng/mL, were used. The extraction recoveries of the FSA-SA derivatives obtained via the OPD/MSPE procedure under varying conditions were juxtaposed against those from the in-solution derivatization method, facilitating the determination of the optimal conditions.

3.2.1. The concentration of FSA

The concentration of the derivatization reagent can influence the efficiency of the derivatization process, which subsequently impacts the extraction efficiency of SAs. In this study, the effect of FSA concentration on the extraction recoveries within a range of 1.0–15.0 mg/mL was examined. As illustrated in Fig. S5A, extraction recoveries increased

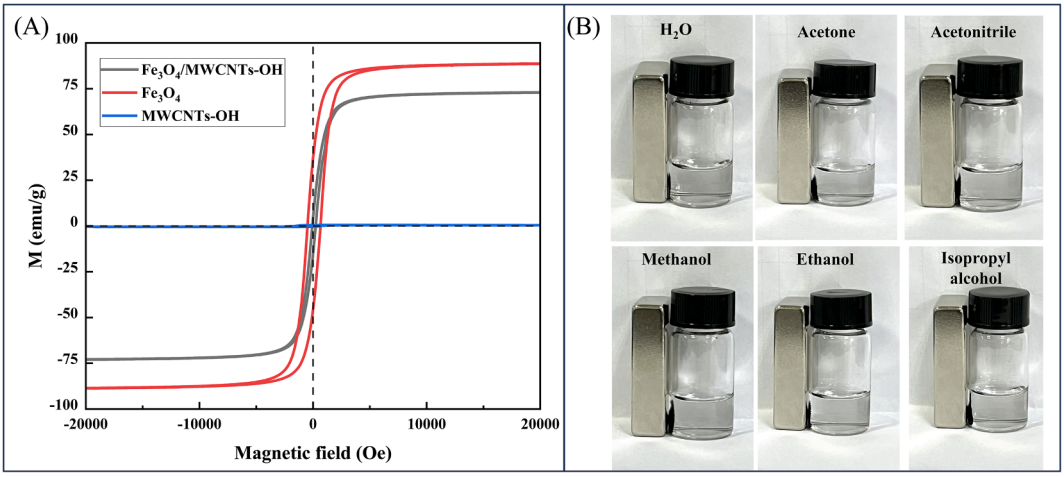

Fig. 3. Characteristics of the sorbent: (A) magnetization curve of Fe_3O_4/MWCNTs-OH and (B) the solid–liquid separation of Fe_3O_4/MWCNTs-OH in different solvents under an applied magnetic field.

with increasing FSA concentrations in ranges of 1.0–10.0 mg/mL. Beyond the threshold concentration of 10.0 mg/mL, the recovery rates reached a plateau. This phenomenon is attributed to the fact that within a specific concentration range, higher concentrations of the derivatization reagent tend to enhance reaction efficiency. However, once the concentration of the derivatization reagent reaches a certain level, the efficiency of the derivatization reaction maximizes and does not increase further. Although increases in target analyte recoveries were not significant beyond 10.0 mg/mL, a concentration of 12.0 mg/mL was selected for subsequent experiments. This selection was based not only on recovery but also on factors such as reagent stability, the robustness of the extraction process, and consistent performance across different sample matrices and conditions, ensuring optimal derivatization efficiency and reproducibility.

3.2.2. The pH of buffer solution

According to a prior report (Li et al., 2020), it was found that the derivatization reaction was more efficient under acidic conditions. Consequently, this study sought to explore the effect of varying pH levels in acetate buffer salt solutions on derivatization efficiency. As shown in Fig. S5B, the maximum extraction recoveries for FSA-SAs were achieved at a pH of 3.5 for the buffer salt solution. When the pH exceeded this value, the extraction recoveries showed a marked decline. This decrease was likely because the nucleophilic activity of the primary amine groups towards FSA is at its peak at pH 3.5, which is conducive to reacting with FSA to form the FSA-SA derivative (Derayea et al., 2020). Based on these results, an acetate buffer salt with a pH of 3.5 was chosen for subsequent experiments.

3.2.3. The derivatization/extraction time

To achieve efficient derivatization and extraction, the influence of derivatization/extraction time on the extraction recovery of FSA-SAs was studied over a range of 1–10 min. As depicted in Fig. S5C, the peak extraction recoveries for FSA-SAs occurred at a vortexing duration of 2 min. No significant improvements in extraction recoveries were noted with longer vortexing times. This observation could be attributed to the fact that reaching extraction equilibrium and achieving maximum derivatization efficiency required a certain amount of time. The results of this experiment suggested that both extraction and derivatization can attain equilibrium within 2 min. To minimize potential errors from factors like human intervention, a vortexing duration of 3 min was chosen for subsequent derivatization/extraction procedures.

3.2.4. The amount of sorbent

The influence of the amount of Fe_3O_4/MWCNTs-OH on the extraction efficiency was explored over a range of 2–10 mg, as depicted in Fig. S5D. The results indicated a significant increase in extraction recoveries of the derivatives as the amount of sorbent material increased from 2.0 mg to 4.0 mg. However, beyond 4.0 mg, no additional improvements in extraction recoveries were observed. This trend could be attributed to the limited adsorption sites available at lower sorbent quantities, which were insufficient to adsorb all FSA-SA derivatives. At and above 4.0 mg, the sorbent provided adequate adsorption sites for the FSA-SA derivatives. Increasing the amount of material beyond this point did not contribute to further enhancement in extraction efficiency, suggesting that 4 mg was enough for maximum adsorption capacity. However, to ensure thorough adsorption of the target analytes without undue interference, an amount of 5.0 mg of Fe_3O_4/MWCNTs-OH was chosen for subsequent experiments.

3.2.5. The type of desorption solvent

In this study, commonly used organic solvents in the laboratory (acetone, acetonitrile, and methanol) were chosen as desorbing solvents to investigate their effects on extraction recoveries. As shown in Fig. S5E, acetone emerged as the most effective solvent, yielding the highest extraction recoveries. The enhanced performance of acetone may potentially be attributed to its ability to disrupt the hydrophobic and π-π interactions, which are thought to primarily govern the adsorption of FSA-SA derivatives by Fe_3O_4/MWCNTs-OH (Rakhtshah et al., 2021; Wang et al., 2017). Therefore, acetone was selected as the desorption solvent for subsequent experiments.

In current study, the desorption solution was directly transferred to LC-FLD analysis for convenience. However, when using acetone as the desorption solvent, phenomenon such as peak splitting and retention time drift, caused by solvent effects, occurred because the elution strength of the sample solvent was greater than the elution strength of the initial mobile phase. This was especially true for the chromatographic peak of FSA labeled SGN, making the analysis less robust. Typically, two strategies can be employed: blow drying the desorption solution and reconstitution in mobile phase, or dilution the desorption solution with water. To simplify the sample preparation process, the desorption solution was diluted one-fold with water before LC-FLD analysis.

3.2.6. The desorption time

The desorption time has the potential to affect the extraction recoveries of the derivatives. In this experiment, the effect of desorption time on the extraction recoveries of FSA-SAs was examined within the range of 1–10 min. The results, presented in Fig. S5F, indicated that the recoveries remained consistent regardless of the desorption time. This consistency might be attributed to the rapid achievement of desorption equilibrium within the first minute, suggesting that the desorption of FSA-SAs from Fe_3O_4/MWCNTs-OH occurs swiftly and efficiently. To ensure complete desorption of the derivatives, a desorption time of 2 min was chosen as the final duration.

3.2.7. The volume of desorption solvent

Next, the effect of acetone volume on the extraction recovery was examined within the range of 100–500 μL. As shown in Fig. S6A, the extraction recovery increased with the volume of the desorption solvent. Considering that the desorption solution was directly analyzed by LC-FLD, the concentrations of derivatives in the desorption solution determine the detection sensitivity. Therefore, the effect of acetone volume on the peak areas of the derivatives was also investigated. The results shown in Fig. S6B indicated that the peak areas of the derivatives decreased as the acetone volume increased. This phenomenon can be attributed to the dilution effect; as the desorption volume increases, the concentration of the FSA-SA derivatives in the solution decreases. Although the efficiency of desorption improves with larger volumes, this increase is insufficient to offset the dilution effect caused by the increased volume, resulting in a reduced concentration of derivatives and, consequently, a lower signal response. Therefore, to achieve higher detection sensitivity, a volume of 100 μL of acetone was chosen as the desorption solvent for subsequent experiments.

3.3. Stability of FSA-SA derivatives

During the experiments, the stability of the FSA-SA derivatives at room temperature was found to be short-lived. To investigate their stability, the derivatives were stored at room temperature (25 °C) and at low temperature (4 °C) over a period of time. The results, presented in Fig. S6A, indicate that the derivatives were relatively stable for up to 2 h at room temperature, after which there was a significant decrease in the response values over time. In contrast, when stored at 4 °C, the derivatives maintained better stability for up to 12 h (Fig. S6B). Based on these findings, it is recommended to maintain the autosampler temperature at 4 °C to ensure accurate quantitative analysis of SAs.

3.4. Potential exaction mechanism

Based on existing research (Chen et al., 2023), a seven-ring pure graphene structure was used to simulate the MWCNTs-OH model. The

structural models of MWCNTs-OH, SD, and MWCNTs-OH@SD were constructed using Gaussian 09 software and investigated using dispersion-corrected density functional theory (DFT-D3(BJ) and D3 with Becke–Johnson damping). The geometry optimization was performed using the B3LYP level of theory and the 6-31G(d) basis set. The binding energy between MWCNTs-OH and SD was calculated using the following equation. Here, ΔE represents the binding energy, EAB represents the energy of the complex, and EA and EB represent the energies of MWCNTs-OH and SD, respectively. After calculation, the binding energy between MWCNTs-OH and SD was found to be −0.0331 eV, indicating the effective adsorption of MWCNTs-OH.

$$\Delta E = E_{AB} - E_A - E_B \quad (1)$$

To further analyze the weak interactions between MWCNTs-OH and SD, the Interaction Region Indicator (IRI) (Lu et al., 2021) and Reduced Density Gradient (RDG) (Johnson et al., 2010) were computed using Multiwfn 3.8 (Lu et al., 2012) and the VMD program (Humphrey et al., 1996). The results, as shown in Fig. S7, reveal prominent basin-shaped green isosurfaces over a large area, indicating the presence of vdW interactions and dispersion-dominated pi-H interactions. Additionally, blue-green isosurfaces are observed, suggesting the existence of O—H interactions between MWCNTs-OH and SD. In the RDG scatter plot, clear scattering near RDG −0.022 a.u. distinctly demonstrates the presence of weak hydrogen bonds (Fan et al., 2022).

3.5. Matrix effects

The complex matrix present in actual samples can interfere with the detection of target analytes. In this study, blank honey samples were spiked with 2.0 ng/mL of SAs to investigate matrix effects. The matrix effect was determined by calculating the ratio of the peak area of the derivatives obtained from the spiked sample to the peak area of the derivatives from the standard aqueous solution of the same concentration. The results, presented in Table S1, indicated that the matrix affected the detection of most SAs. However, the recoveries of each analyte across the three different types of honey samples were comparable. Consequently, any of the honey samples were subsequently chosen as blank matrices for method validation.

3.6. Method validation

Under the optimized experimental conditions, calibration curves were constructed by plotting the chromatographic peak areas against the respective analyte concentrations, and linear regressions were performed. As presented in Table 1, the calibration curves exhibited satisfactory linearity for all SAs, with regression coefficients (R^2) exceeding 0.99. The limits of detection (LODs) were determined based on a signal-to-noise ratio of 3:1 and ranged from 0.004 to 0.04 ng/g.

Table 1
Calibration curves, LOQs and LODs of SAs in honey obtained by OPD/MSPE method.

SAs	Regression line		(R^2)	LODs (ng/g)	LOQs (ng/g)
	Linear range (ng/g)	Linear equation			
SGN	0.10–10.0	y = 240197x − 2066	0.9992	0.04	0.12
SA	0.05–10.00	y = 453920x − 1085	0.9990	0.02	0.06
SDZ	0.05–10.00	y = 613892x + 2339	0.9990	0.02	0.06
SMZ	0.05–10.00	y = 396362x + 3261	0.9991	0.02	0.06
SMM	0.05–10.00	y = 458010x − 4776	0.9994	0.02	0.06
SMD	0.05–10.00	y = 596685x − 8638	0.9996	0.02	0.06
SMX	0.02–10.00	y = 881265x + 2371	0.9995	0.01	0.03
SDM	0.02–10.00	y = 514962x + 3520	0.9995	0.01	0.03
SB	0.01–10.00	y = 2281448x + 6720	0.9989	0.004	0.012

The accuracy and precision of the validated method were assessed through relative recoveries and intra- and inter-day relative standard deviations (RSDs). The blank honey sample was spiked with SAs at low (0.1 ng/g), medium (1 ng/g), and high (8 ng/g) concentrations, and three replicates were performed to calculate the relative recoveries and RSDs. As indicated in Table S2, the relative recoveries ranged from 86.2 % to 111.2 %, with intra-day and inter-day RSDs below 10.5 %. These results demonstrate that the method exhibited satisfactory accuracy and precision for quantitative analysis.

3.7. Applications towards real sample

SAs have long been used in the beekeeping sector to counteract common bacterial larval diseases like American foulbrood and European foulbrood, playing a key role in reducing bee fatalities (Kadziński et al., 2018; Zhang et al., 2021). However, due to the slow metabolism and degradation of sulfonamides in animals, excessive unauthorized use could lead to their residue in bees and consequently in bee products. As early as 2003, China issued a standard for SA residues in honey, GB/T 18932.17-2003, which is still the current standard. The multi-drug residue standard for honey, GB/T 22943-2008, established in 2008, also includes SA residues. Thus, determination of SAs in honey is crucial as a precautionary measure to ensure consumer safety.

In this study, the validated OPD/MSPE method was applied to determine SAs in five real honey samples to gauge its practical applicability. No SAs were detected in any of the samples. The inability to detect these residues is largely attributed to the limited sample size (only five honey samples) and increasingly stringent market regulation. To further assess the method's quantitative analysis capability, a single-blind method was employed [37]. This involved analyzing five honey samples spiked with unknown concentrations of SAs, with the spiked levels concealed from the operator until the final assay results were disclosed. The results, presented in Table S3, showed that the detection levels closely matched the spiked levels, indicating that the method's effectiveness for accurate analysis of sulfonamides in real samples.

3.8. Comparisons with reported methods

The proposed method was compared with other reported method for detecting SAs in different samples (Table 2). Compared with the methods reported in references [37–40], the OPD/MSPE method developed in this study offers several advantages. Firstly, it integrates the derivatization and extraction steps into a single process, allowing for simultaneous derivatization and extraction. This integration simplifies and speeds up the analysis procedure, making it more straightforward and efficient. Secondly, rapid phase separation is achieved using an external magnet, eliminating the need for centrifugation and further streamlining the sample pretreatment process. The entire preparation process takes only 5 min. Thirdly, many detection instruments, such as LC-UV, exhibit low selectivity for SAs, often resulting in interference due to overlapping absorption wavelengths between sulfonamides (around 270–280 nm) and proteins in animal tissues (around 280 nm). In this study, fluorescence derivatization of SAs was employed, enhancing detection specificity and reducing the method's detection limit. In summary, when combined with LC-FLD, the OPD/MSPE method developed in this study offers a strategy characterized by simplicity, speed, high sensitivity, and high specificity for analytically detecting sulfonamides in complex matrix samples.

4. Conclusion

In this paper, a simple, rapid, and efficient method named one-pot derivatization/magnetic solid-phase extraction (OPD/MSPE) has been developed for the purification and enrichment of sulfonamides in complex samples. This method, combined with LC-FLD, establishes a qualitative and quantitative analysis technique for nine sulfonamides in

Table 2
Comparisons of proposed method with previous reported methods for the determination of SAs.

Sample	Sample preparation	Detection	LODs	Sample preparation time	Ref
Organic fertilizers	Derivatization and SPE	LC-FLD	15.53–23.30 ng/g	~15 min	(Osiński et al., 2022)
Feeds	Derivatization and SPE	LC-FLD	34.50–79.50 ng/g	~15 min	(Patyra et al., 2019)
Milk	DLLME or QuEChERS	LC-FLD	1.22–2.73 ng/mL DLLME: 0.89–1.21 ng/mL; QuEChERS:	~20 min	(Arroyo-Manzanares et al., 2014)
Environment water	SALLME	LC-UV	2.15–7.64 ng/mL	~8 min	(Mokhtar et al., 2019)
Honey, milk	MIT	LC-UV	0.39–0.47 ng/g	~60 min	(Wang et al., 2022)
Honey, milk	PT-SPE	LC-UV	9.50–16.50 ng/mL	~50 min	(Sadeghi et al., 2019)
Honey	OPD/MSPE	LC-FLD	0.004–0.04 ng/g	~5 min	This work

honey. The OPD/MSPE method integrates the derivatization and extraction steps into a single procedure, and phase separation is achieved using an external magnet. This approach streamlines the sample pretreatment process, making it both easier and faster, with the entire preparation process completed in just 5 min. The OPD/MSPE method boasts advantages such as simplicity, speed, high sensitivity, specificity, and minimal use of organic solvents. It presents a new avenue for the pretreatment of complex samples.

CRediT authorship contribution statement

Nian Shi: Writing – original draft, Methodology, Funding acquisition. **Yuwei Liu:** Methodology. **Wenxuan Li:** Methodology. **Shumei Yan:** Writing – review & editing. **Lei Ma:** Writing – review & editing. **Xia Xu:** Writing – review & editing. **Di Chen:** Writing – review & editing, Conceptualization.

Declaration of competing interest

The authors declare that they have no known competing financial interests or personal relationships that could have appeared to influence the work reported in this paper.

Data availability

Data will be made available on request.

Acknowledgements

The authors thank the financial support from the Henan Province Medical Science and Technology Research Project jointly built by the Ministry and Province (LHGJ20220392) and the Key Scientific Research Projects of Universities in Henan Province (23A320044).

Appendix A. Supplementary data

Supplementary data to this article can be found online at https://doi.org/10.1016/j.fochx.2023.101090.

References

Arroyo-Manzanares, G.-G., & García-Campaña. (2014). Alternative sample treatments for the determination of sulfonamides in milk by HPLC with fluorescence detection. *Food Chemistry, 143*, 459–464. https://doi.org/10.1016/j.foodchem.2013.08.008

Fonte, B., Castro, R., & Liva-Garrido. (2018). Multi-residue analysis of sulfonamide antibiotics in honey samples by on-line solid phase extraction using molecularly imprinted polymers coupled to liquid chromatography-tandem mass spectrometry. *Journal of Liquid Chromatography & Related Technologies, 41*(15–16), 881–891. https://doi.org/10.1080/10826076.2018.1533477

Bonerba, P., Arioli, N., Terio, D. C., Tantillo, & Maria Chiesa. (2021). Determination of antibiotic residues in honey in relation to different potential sources and relevance for food inspection. *Food Chemistry, 334*, Article 127575. https://doi.org/10.1016/j.foodchem.2020.127575

Cao, X.u., Xue, F., & Zhang. (2019). An in situ derivatization combined with magnetic ionic liquid-based fast dispersive liquid-liquid microextraction for determination of biogenic amines in food samples. *Talanta, 199*, 212–219. https://doi.org/10.1016/j.talanta.2019.02.065

Chen, C., Du, W.u., Tao, Z., Dang, & Lu. (2023). Adsorption behavior of hierarchical porous biochar from shrimp shell for tris(2-chloroethyl) phosphate (TCEP): Sorption experiments and DFT calculations. *Environmental Research, 219*, Article 115128. https://doi.org/10.1016/j.envres.2022.115128

Chen, & Xie. (2018). Overview of sulfonamide biodegradation and the relevant pathways and microorganisms. *Science of the Total Environment, 640*, 1465–1477. https://doi.org/10.1016/j.scitotenv.2018.06.016

Dai, W.u., Liu, Y.u., Wu, & Jian. (2023). Simple and efficient solid phase extraction based on molecularly imprinted resorcinol–formaldehyde resin nanofibers for determination of trace sulfonamides in animal-origin foods. *Food Chemistry, 404*, Article 134671. https://doi.org/10.1016/j.foodchem.2022.134671

Derayea, & Samir. (2020). A review on the use of fluorescamine as versatile and convenient analytical probe. *Microchemical Journal, 156*, Article 104835. https://doi.org/10.1016/j.microc.2020.104835

Dmitrienko, K., Tolmacheva, A., & Zolotov. (2015). Determination of the total content of some sulfonamides in milk using solid-phase extraction coupled with off-line derivatization and spectrophotometric detection. *Food Chemistry, 188*, 51–56. https://doi.org/10.1016/j.foodchem.2015.04.123

Duan, C., Jia, & Huang. (2022). Occurrence and ecotoxicity of sulfonamides in the aquatic environment: A review. *Science of the Total Environment, 820*, Article 153178. https://doi.org/10.1016/j.scitotenv.2022.153178

Fan, L.u., Li, D.u., Huang, M.a., Wang, T., Dang, & Lu. (2022). Efficient removal of organophosphate esters by ligand functionalized MIL-101 (Fe): Modulated adsorption and DFT calculations. *Chemosphere, 302*, Article 134881. https://doi.org/10.1016/j.chemosphere.2022.134881

Humphrey, D., & Schulten. (1996). VMD: Visual molecular dynamics. *Journal of Molecular Graphics, 14*(1), 33–38. https://doi.org/10.1016/0263-7855(96)00018-5

Johnson, K., Mori-Sánchez, C.-G., Cohen, & Yang. (2010). Revealing Noncovalent Interactions. *Journal of the American Chemical Society, 132*(18), 6498–6506. https://doi.org/10.1021/ja100936w

Kadziński, B., & Banecki. (2018). Determination of ten sulfonamides in honey using tetrahydrofuran Salting Out Liquid Liquid Extraction and monolithic silica column. *LWT, 96*, 7–12. https://doi.org/10.1016/j.lwt.2018.05.007

Li, Z.u., Zhang, L.i., Iqbal, W.u., & Du. (2020). Rapid detection of sulfamethoxazole in plasma and food samples with in-syringe membrane SPE coupled with solid-phase fluorescence spectrometry. *Food Chemistry, 320*, Article 126612. https://doi.org/10.1016/j.foodchem.2020.126612

Lu, & Chen. (2012). Multiwfn: A multifunctional wavefunction analyzer. *33*(5), 580-592. https://doi.org/10.1002/jcc.22885.

Lu, & Chen. (2021). Interaction Region Indicator: A Simple Real Space Function. *Clearly Revealing Both Chemical Bonds and Weak Interactions**., *1*(5), 231–239. https://doi.org/10.1002/cmtd.202100007

Luo, X.u., Wang, L., Huang, & Xiao. (2021). Magnetic Ti3C2 MXene functionalized with beta-cyclodextrin as magnetic solid-phase extraction and in situ derivatization for determining 12 phytohormones in oilseeds by ultra-performance liquid chromatography-tandem mass spectrometry. *Phytochemistry, 183*, Article 112611. https://doi.org/10.1016/j.phytochem.2020.112611

Mokhtar, A.-S., & Hadad. (2019). Tolerance intervals modeling for design space of a salt assisted liquid-liquid microextraction of trimethoprim and six common sulfonamide antibiotics in environmental water samples. *Journal of Chromatography A, 1586*, 18–29. https://doi.org/10.1016/j.chroma.2018.12.003

Ning, Y.e., Liao, X.u., Wang, & Wang. (2022). Triazine-based porous organic polymer as pipette tip solid-phase extraction adsorbent coupled with HPLC for the determination of sulfonamide residues in food samples. *Food Chemistry, 397*, Article 133831. https://doi.org/10.1016/j.foodchem.2022.133831

Osiński, P., & Kwiatek. (2022). HPLC-FLD-based method for the detection of sulfonamides in organic fertilizers collected from poland. *Molecules, 27*(6), 2–12. https://doi.org/10.3390/molecules27062031

Patyra, P.-S., & Kwiatek. (2019). Determination of sulfonamides in feeds by high-performance liquid chromatography after fluorescamine precolumn derivatization. *Molecules, 24*(3), 452–456. https://doi.org/10.3390/molecules24030452

Rakhtshah, S., & Esmaeili. (2021). A rapid extraction of toxic styrene from water and wastewater samples based on hydroxyethyl methylimidazolium tetrafluoroborate immobilized on MWCNTs by ultra-assisted dispersive cyclic conjugation-micro-solid phase extraction. *Microchemical Journal, 170*, Article 106759. https://doi.org/10.1016/j.microc.2021.106759

Sadeghi, & Olieaei. (2019). Nanostructured polyaniline based pipette tip solid phase extraction coupled with high-performance liquid chromatography for the selective determination of trace levels of three sulfonamides in honey and milk samples with the aid of experimental design methodology. *Microchemical Journal, 146*, 974–985. https://doi.org/10.1016/j.microc.2019.02.020

Wang, H.e., Zhang, T., Xu, Z., Li, C., & He. (2022). Application of magnetic hydroxyapatite surface-imprinted polymers in pretreatment for detection of zearalenone in cereal samples. *Journal of Chromatography B, 1201–1202*, Article 123297. https://doi.org/10.1016/j.jchromb.2022.123297

Wang, M.a., Si, D., Wang, Y., Chen, Y.i., Yao, & Xing. (2017). Interaction mechanisms of antibiotic sulfamethoxazole with various graphene-based materials and multiwall carbon nanotubes and the effect of humic acid in water. *Carbon, 114*, 671–678. https://doi.org/10.1016/j.carbon.2016.12.080

Xie, H., Zheng, & Ouyang. (2020). Trends in sensitive detection and rapid removal of sulfonamides: A review. *Journal of Separation Science, 43*(9–10), 1634–1652. https://doi.org/10.1002/jssc.201901341

Yang, S., Li, & Luan. (2018). In situ derivatization and hollow-fiber liquid-phase microextraction to determine sulfonamides in water using UHPLC with fluorescence detection. *Journal of Separation Science, 41*(7), 1651–1662. https://doi.org/10.1002/jssc.201701041

Zhang, L.i., Guo, Z., Li, L.i., Jiao, & Zhang. (2021). Assessment of the impact of hydrolysis on bound sulfonamide residue determination in honey using stable isotope dilution ultrahigh performance liquid chromatography tandem mass spectrometry. *Food Chemistry, 361*, Article 130094. https://doi.org/10.1016/j.foodchem.2021.130094

Zhang, L.i., Li, Z., Gao, & Li. (2019). Antibiotic residues in honey: A review on analytical methods by liquid chromatography tandem mass spectrometry. *TrAC Trends in Analytical Chemistry, 110*, 344–356. https://doi.org/10.1016/j.trac.2018.11.015

Zheng, D., Zheng, Z.u., Yuan, & Feng. (2016). Facile synthesis of magnetic carbon nitride nanosheets and its application in magnetic solid phase extraction for polycyclic aromatic hydrocarbons in edible oil samples. *Talanta, 148*, 46–53. https://doi.org/10.1016/j.talanta.2015.10.059